

Cite this: *J. Mater. Chem.*, 2011, **21**, 9938www.rsc.org/materials

FEATURE ARTICLE

A review of advanced and practical lithium battery materials

Rotem Marom,* S. Francis Amalraj, Nicole Leifer, David Jacob and Doron Aurbach

Received 3rd December 2010, Accepted 31st January 2011

DOI: 10.1039/c0jm04225k

Presented herein is a discussion of the forefront in research and development of advanced electrode materials and electrolyte solutions for the next generation of lithium ion batteries. The main challenge of the field today is in meeting the demands necessary to make the electric vehicle fully commercially viable. This requires high energy and power densities with no compromise in safety. Three families of advanced cathode materials (the limiting factor for energy density in the Li battery systems) are discussed in detail: $\text{LiMn}_{1.5}\text{Ni}_{0.5}\text{O}_4$ high voltage spinel compounds, Li_2MnO_3 – LiMO_2 high capacity composite layered compounds, and LiMPO_4 , where $\text{M} = \text{Fe}, \text{Mn}$. Graphite, Si, Li_xTO_y , and MO (conversion reactions) are discussed as anode materials. The electrolyte is a key component that determines the ability to use high voltage cathodes and low voltage anodes in the same system. Electrode–solution interactions and passivation phenomena on both electrodes in Li-ion batteries also play significant roles in determining stability, cycle life and safety features. This presentation is aimed at providing an overall picture of the road map necessary for the future development of advanced high energy density Li-ion batteries for EV applications.

Introduction

One of the greatest challenges of modern society is to stabilize a consistent energy supply that will meet our growing energy demands. A consideration of the facts at hand related to the energy sources on earth reveals that we are not encountering an energy crisis related to a shortage in total resources. For instance

the earth's crust contains enough coal for the production of electricity for hundreds of years.¹ However the continued unbridled usage of this resource as it is currently employed may potentially bring about catastrophic climatological effects. As far as the availability of crude oil, however, it in fact appears that we are already beyond 'peak' production.² As a result, increasing oil shortages in the near future seem inevitable. Therefore it is of critical importance to considerably decrease our use of oil for propulsion by developing effective electric vehicles (EVs). EV applications require high energy density energy storage devices that can enable a reasonable driving range between

Department of Chemistry, Bar-Ilan University, Ramat-Gan, 52900, Israel;
Web: <http://www.ch.biu.ac.il/people/aurbach>. E-mail: rotem.marom@live.biu.ac.il; aurbach@mail.biu.ac.il



Rotem Marom

Rotem Marom received her BS degree in organic chemistry (2005) and MS degree in polymer chemistry (2007) from Bar-Ilan University, Ramat Gan, Israel. She started a PhD in electrochemistry under the supervision of Prof. D. Aurbach in 2010. She is currently conducting research on a variety of lithium ion battery materials for electric vehicles, with a focus on electrolyte solutions, salts and additives.



S. Francis Amalraj

Francis Amalraj hails from Tamil Nadu, India. He received his MSc in Applied Chemistry from Anna University. He then carried out his doctoral studies at National Chemical Laboratory, Pune and obtained his PhD in Chemistry from Pune University (2008). He is currently a postdoctoral fellow in Prof. Doron Aurbach's group at Bar-Ilan University, Israel. His current research interest focuses on the synthesis, electrochemical and transport properties of high energetic electrode materials for energy conversion and storage systems.

charges and maintain acceptable speeds.³ Other important requirements are high power density and acceptable safety features. The energy storage field faces a second critical challenge: namely, the development of rechargeable systems for load leveling applications (e.g. storing solar and wind energy, and reducing the massive wasted electricity from conventional fossil fuel combustion plants).⁴ Here the main requirements are a very prolonged cycle life, components (*i.e.*, relevant elements) abundant in high quantities in the earth's crust, and environmentally friendly systems. Since it is not clear whether Li-ion battery technology can contribute significantly to this application, battery-centered solutions for this application are not discussed



Nicole Leifer

Nicole Leifer received a BS degree in chemistry from MIT in 1998. After teaching high school chemistry and physics for several years at Stuyvesant High School in New York City, she began work towards her PhD in solid state physics from the City University of New York Graduate Center. Her research consisted primarily of employing solid state NMR in the study of lithium ion electrode materials and electrode surface phenomena with Prof. Greenbaum at Hunter College and

Prof. Grey at Stony Brook University. After completing her PhD she joined Prof. Doron Aurbach for a postdoctorate at Bar-Ilan University to continue work in lithium ion battery research. There she continues her work in using NMR to study lithium materials in addition to new forays into carbon materials' research for super-capacitor applications with a focus on enhancement of electrochemical performance through the incorporation of carbon nanotubes.



David Jacob

David Jacob earned a BSc from Amravati University in 1998, an MSc from Pune University in 2000, and completed his PhD at Bar-Ilan University in 2007 under the tutelage of Professor Aharon Gedanken. As part of his PhD research, he developed novel methods of synthesizing metal fluoride nano-material structures in ionic liquids. Upon finishing his PhD he joined Prof. Doron Aurbach's lithium ion battery group at Bar-Ilan in 2007 as a post-doctorate and during that time developed new

formulations of electrolyte solutions for Li-ion batteries. He has a great interest in nanotechnology and as of 2011, has become the CEO of IsraZion Ltd., a company dedicated to the manufacturing of novel nano-materials.

herein. In fact, even for electrical propulsion, the non-petroleum power source with the highest energy density is the H₂/O₂ fuel cell (FC).⁵ However, despite impressive developments in recent years in the field, there are intrinsic problems related to electrocatalysis in the FCs and the storage of hydrogen⁶ that will need many years of R&D to solve. Hence, for the foreseeable future, rechargeable batteries appear to be the most practically viable power source for EVs. Among the available battery technologies to date, only Li-ion batteries may possess the power and energy densities necessary for EV applications.

The commonly used Li-ion batteries that power almost all portable electronic equipment today are comprised of a graphite anode and a LiCoO₂ cathode (3.6 V system) and can reach a practical energy density of 150 W h kg⁻¹ in single cells. This battery technology is not very useful for EV application due to its limited cycle life (especially at elevated temperatures) and problematic safety features (especially for large, multi-cell modules).⁷ While there are ongoing developments in the hybrid EV field, including practical ones in which only part of the propulsion of the car is driven by an electrical motor and batteries,⁸ the main goal of the battery community is to be able to develop full EV applications. This necessitates the development of Li-ion batteries with much higher energy densities compared to the practical state-of-the-art. The biggest challenge is that Li-ion batteries are complicated devices whose components never reach thermodynamic stability. The surface chemistry that occurs within these systems is very complicated, as described briefly below, and continues to be the main factor that determines their performance.⁹



Doron Aurbach

Dr Doron Aurbach is a full Professor in the Department of Chemistry at Bar-Ilan University (BIU) in Ramat Gan, Israel and a senate member at BIU since 1996. He chaired the chemistry department there during the years 2001–2005. He is also the chairman of the Israeli Labs Accreditation Authority. He founded the electrochemistry group at BIU at the end of 1985. His group conducts research in the following fields: Li ion batteries for electric vehicles and for other

portable uses (new cathodes, anodes, electrolyte solutions, electrodes–solution interactions, practical systems), rechargeable magnesium batteries, electronically conducting polymers, super-capacitors, engineering of new carbonaceous materials, development of devices for storage and conversion of sustainable energy (solar, wind) sensors and water desalination. The group currently collaborates with several prominent research groups in Europe and the US and with several commercial companies in Israel and abroad. He is also a fellow of the ECS and ISE as well as an associate editor of Electrochemical and Solid State Letters and the Journal of Solid State Electrochemistry. Prof. Aurbach has more than 350 journals publications.

All electrodes, excluding 1.5 V systems such as LiTiO_x anodes, are surface-film controlled (SFC) systems. At the anode side, all conventional electrolyte systems can be reduced in the presence of Li ions below 1.5 V, thus forming insoluble Li-ion salts that comprise a passivating surface layer of particles referred to as the solid electrolyte interphase (SEI).¹⁰ The cathode side is less trivial. Alkyl carbonates can be oxidized at potentials below 4 V.¹¹ These reactions are inhibited on the passivated aluminium current collectors (Al CC) and on the composite cathodes. There is a rich surface chemistry on the cathode surface as well. In their lithiated state, nucleophilic oxygen anions in the surface layer of the cathode particles attack electrophilic $\text{RO}(\text{CO})\text{OR}$ solvents, forming different combinations of surface components (e.g. ROCO_2Li , ROCO_2M , ROLi , ROM etc.) depending on the electrolytes used.¹² The polymerization of solvent molecules such as EC by cationic stimulation results in the formation of polycarbonates.¹³ The dissolution of transition metal cations forms surface inactive Li_xMO_y phases.¹⁴ Their precipitation on the anode side destroys the passivation of the negative electrodes.¹⁵ Red-ox reactions with solution species form inactive LiMO_y with the transition metal M at a lower oxidation state.¹⁴ LiMO_y compounds are spontaneously delithiated in air due to reactions with CO_2 .¹⁶ Acid-base reactions occur in the LiPF_6 solutions (trace HF, water) that are commonly used in Li-ion batteries. Finally, LiCoO_2 itself has a rich surface chemistry that influences its performance:



Co^{III} compounds oxidize alkyl carbonates; CO_2 is one of the products, $\text{Co}^{\text{III}} \rightarrow \text{Co}^{\text{II}} \rightarrow \text{Co}^{2+}$ dissolution.¹⁴

Interestingly, this process seems to be self-limiting, as the presence of Co^{2+} ions in solution itself stabilizes the LiCoO_2 electrodes.¹⁷ However, Co metal in turn appears to deposit on the negative electrodes, destroying their passivation.

Hence the performance of many types of electrodes depends on their surface chemistry. Unfortunately surface studies provide more ambiguous results than bulk studies, therefore there are still many open questions related to the surface chemistry of Li-ion battery systems.

It is for these reasons that proper R&D of advanced materials for Li-ion batteries has to include bulk structural and performance studies, electrode-solution interactions, and possible reflections between the anode and cathode. These studies require the use of the most advanced electrochemical,¹⁸ structural (XRD, HR microscopy), spectroscopic and surface sensitive analytical techniques (SS NMR,¹⁹ FTIR,²⁰ XPS,²¹ Raman,²² X-ray based spectroscopies²³). This presentation provides a review of the forefront of the study of advanced materials—electrolyte systems, current collectors, anode materials, and finally advanced cathodes materials used in Li-ion batteries, with the emphasis on contributions from the authors' group.

Experimental

Many of the materials reviewed were studied in this laboratory, therefore the experimental details have been provided as follows. The LiMO_2 compounds studied were prepared *via* self-combustion reactions (SCRs).²⁴ $\text{Li}[\text{MnNiCo}]\text{O}_2$ and $\text{Li}_2\text{MnO}_3 \cdot \text{Li}/\text{MnNiCo}]\text{O}_2$ materials were produced in nano- and

submicrometric particles both produced by SCR with different annealing stages (700 °C for 1 hour in air, 900 °C or 1000 °C for 22 hours in air, respectively). $\text{LiMn}_{1.5}\text{Ni}_{0.5}\text{O}_4$ spinel particles were also synthesized using SCR. $\text{Li}_4\text{T}_5\text{O}_{12}$ nanoparticles were obtained from NEI Inc., USA. Graphitic material was obtained from Superior Graphite (USA), Timcal (Switzerland), and Conoco-Philips. $\text{LiMn}_{0.8}\text{Fe}_{0.2}\text{PO}_4$ was obtained from HPL Switzerland. Standard electrolyte solutions (alkyl carbonates/ LiPF_6), ready to use, were obtained from UBE, Japan. Ionic liquids were obtained from Merck KGaA (Germany and Toyo Gosei Ltd., (Japan)).

The surface chemistry of the various electrodes was characterized by the following techniques: Fourier transform infrared (FTIR) spectroscopy using a Magna 860 Spectrometer from Nicolet Inc., placed in a homemade glove box purged with H_2O and CO_2 (Balson Inc. air purification system) and carried out in diffuse reflectance mode; high-resolution transmission electron microscopy (HR-TEM) and scanning electron microscopy (SEM), using a JEOL-JEM-2011 (200kV) and JEOL-JSM-7000F electron microscopes, respectively, both equipped with an energy dispersive X-ray microanalysis system from Oxford Inc.; X-ray photoelectron spectroscopy (XPS) using an HX Axis spectrometer from Kratos, Inc. (England) with monochromatic Al K α (1486.6eV) X-ray beam radiation; solid state ^7Li magic angle spinning (MAS) NMR performed at 194.34 MHz on a Bruker Avance 500 MHz spectrometer in 3.2 mm rotors at spinning speeds of 18–22 kHz; single pulse and rotor synchronized Hahn echo sequences were used, and the spectra were referenced to 1 M LiCl at 0 ppm; MicroRaman spectroscopy with a spectrometer from Jobin-Yvon Inc., France. We also used Mössbauer spectroscopy for studying the stability of LiMPO_4 compounds (conventional constant-acceleration spectrometer, room temperature, 50 mC; $^{57}\text{Co}:\text{Rh}$ source, the absorbers were put in Perspex holders. *In situ* AFM measurements were carried out using the system described in ref. 25.

The following electrochemical measurements were conducted. Composite electrodes were prepared by spreading slurries comprising the active mass, carbon powder and poly-vinylidene difluoride (PVdF) binder (ratio of 75% : 15% : 10% by weight, mixed into *N*-methyl pyrrolidone (NMP), and deposited onto aluminium foil current collectors, followed by drying in a vacuum oven. The average load was around 2.5 mg active mass per cm^2 . These electrodes were tested in two-electrode, coin-type cells (Model 2032 from NRC Canada) with Li foil serving as the counter electrode, and various electrolyte solutions. Computerized multi-channel battery analyzers from Maccor Inc. (USA) and Arbin Inc. were used for galvanostatic measurements (voltage vs. time/capacity, measured at constant currents).

Results and discussion

Our road map for materials development

Fig. 1 indicates a suggested road map for the direction of Li-ion research. The axes are voltage and capacity, and a variety of electrode materials are marked therein according to their respective values. As is clear, the main limiting factor is the cathode material (in voltage and capacity). The electrode materials currently used in today's practical batteries allow for

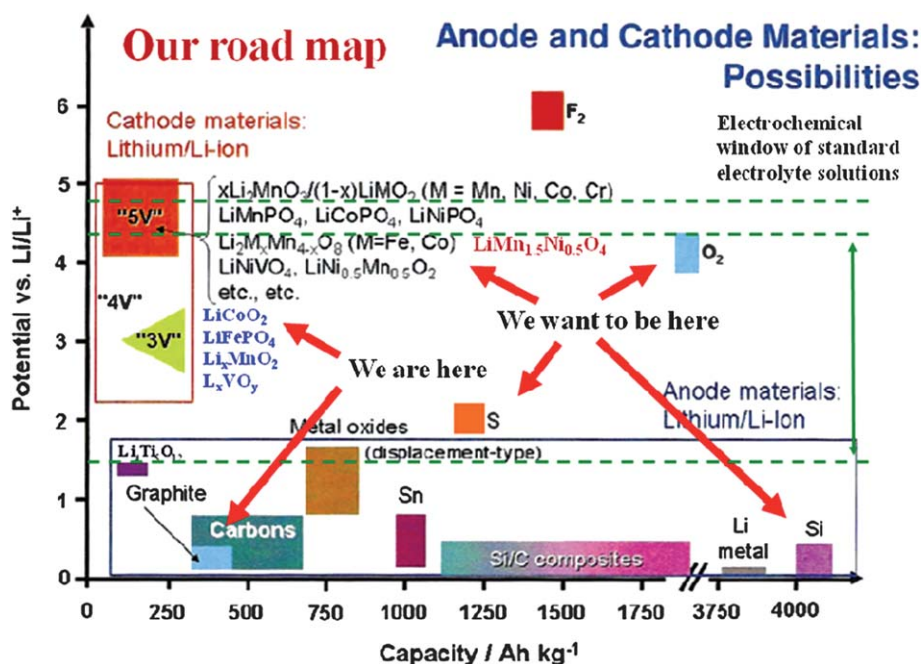


Fig. 1 The road map for R&D of new electrode materials, compared to today's state-of-the-art. The y and x axes are voltage and specific capacity, respectively.

a nominal voltage of below 4 V. The lower limit of the electrochemical window of the currently used electrolyte solutions (alkyl carbonates/LiPF₆) is approximately 1.5 V vs. Li²⁶ (see later discussion about the passivation phenomena that allow for the operation of lower voltage electrodes, such as Li and Li-graphite). The anodic limit of the electrochemical window of the alkyl carbonate/LiPF₆ solutions has not been specifically determined but practical accepted values are between 4.2 and 5 V vs. Li²⁶ (see further discussion). With some systems which will be discussed later, meta-stability up to 4.9 V can be achieved in these standard electrolyte solutions.

Electrolyte solutions

The anodic stability limits of electrolyte solutions for Li-ion batteries (and those of polar aprotic solutions in general) demand ongoing research in this subfield as well. It is hard to define the onset of oxidation reactions of nonaqueous electrolyte solutions because these strongly depend on the level of purity, the presence of contaminants, and the types of electrodes used. Alkyl carbonates are still the solutions of choice with little competition (except by ionic liquids, as discussed below) because of the high oxidation state of their central carbon (+4). Within this class of compounds EC and DMC have the highest anodic stability, due to their small alkyl groups. An additional benefit is that, as discussed above, all kinds of negative electrodes, Li, Li-graphite, Li-Si, *etc.*, develop excellent passivation in these solutions at low potentials.

The potentiodynamic behavior of polar aprotic solutions based on alkyl carbonates and inert electrodes (Pt, glassy carbon, Au) shows an impressive anodic stability and an irreversible cathodic wave whose onset is ~1.5 V vs. Li, which does not appear in consequent cycles due to passivation of the anode surface by

the SEI. The onset of these oxidation reactions is not well defined (>4.5 V vs. Li). An important discovery was the fact that in the presence of Li salts, EC, one of the most reactive alkyl carbonates (in terms of reduction), forms a variety of semi-organic Li-containing salts that serve as passivation agents on Li, Li-carbon, Li-Si, and inert metal electrodes polarized to low potentials. Fig. 2 and Scheme 1 indicates the most significant reduction schemes for EC, as elucidated through spectroscopic measurements (FTIR, XPS, NMR, Raman).^{27–29} It is important to note (as reflected in Scheme 1) that the nature of the Li salts present greatly affects the electrode surface chemistry. When the presence of the salt does not induce the formation of acidic species in solutions (*e.g.*, LiClO₄, LiN(SO₂CF₃)₂), alkyl carbonates are reduced to ROCO₂Li and ROLi compounds, as presented in Fig. 2. In LiPF₆ solutions acidic species are formed: LiPF₆ decomposes thermally to LiF and PF₅. The latter moiety is a Lewis acid which further reacts with any protic contaminants (*e.g.* unavoidably present traces of water) to form HF. The presence of such acidic species in solution strongly affects the surface chemistry in two ways. One way is that PF₅ interacts with

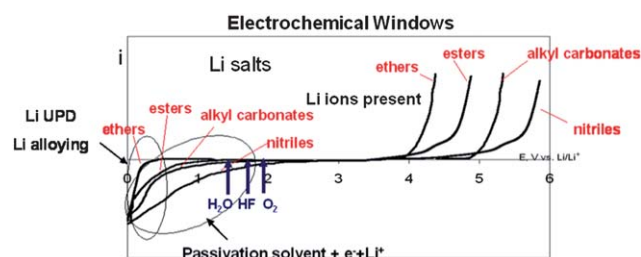
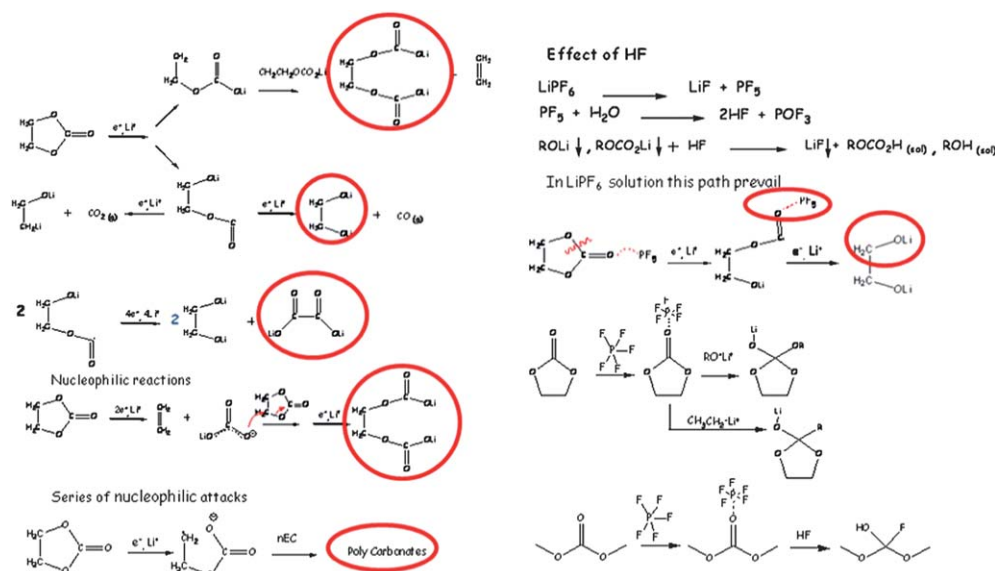


Fig. 2 A schematic presentation of the CV behavior of inert (Pt) electrodes in various families of polar aprotic solvents with Li salts.²⁶



Scheme 1 A reaction scheme for all possible reduction paths of EC that form passivating surface species (detected by FTIR, XPS, Raman, and SSNMR^{28–31,49}).

the carbonyl group and channels the reduction process of EC to form ethylene di-alkoxide species along with more complicated alkoxy compounds such as binary and tertiary ethers, rather than Li-ethylene dicarbonates (see schemes in Fig. 2); the other way is that HF reacts with ROLi and ROCO_2Li to form ROH , ROCO_2H (which further decomposes to ROH and CO_2), and surface LiF . Other species formed from the reduction of EC are Li-oxalate and moieties with Li–C and C–F bonds (see Scheme 1).^{27–31}

Efforts have been made to enhance the formation of the passivation layer (on graphite electrodes in particular) in the presence of these solutions through the use of surface-active additives such as vinylene carbonate (VC) and lithium bi-oxalato borate (LiBOB).²⁷ At this point there are hundreds of publications and patents on various passivating agents, particularly for graphite electrodes; their further discussion is beyond the scope of this paper. Readers may instead be referred to the excellent review by Xu³² on this subject.

Ionic liquids (ILs) have excellent qualities that could render them very relevant for use in advanced Li-ion batteries, including high anodic stability, low volatility and low flammability. Their main drawbacks are their high viscosities, problems in wetting particle pores in composite structures, and low ionic conductivity at low temperatures. Recent years have seen increasing efforts to test ILs as solvents or additives in Li-ion battery systems.³³

Fig. 3 shows the cyclic voltammetric response (Pt working electrodes) of imidazolium-, piperidinium-, and pyrrolidinium-based ILs with $\text{N}(\text{SO}_2\text{CF}_3)_2^-$ anions containing $\text{LiN}(\text{SO}_2\text{CF}_3)_2$ salt.³⁴ This figure reflects the very wide electrochemical window and impressive anodic stability (>5 V) of piperidinium- and pyrrolidinium-based ILs. Imidazolium-based IL solutions have a much lower cathodic stability than the above cyclic quaternary ammonium cation-based IL solutions, as demonstrated in Fig. 3. The cyclic voltammograms of several common electrode materials measured in IL-based solutions are also included in the figure. It is clearly demonstrated that the Li, Li–Si, LiCoO_2 , and

$\text{LiMn}_{1.5}\text{Ni}_{0.5}\text{O}_4$ electrodes behave reversibly in piperidinium- and pyrrolidinium-based ILs with $\text{N}(\text{SO}_2\text{CF}_3)_2^-$ and $\text{LiN}(\text{SO}_2\text{CF}_3)_2$ salts. This figure demonstrates the main advantage of the above IL systems: namely, the wide electrochemical window with exceptionally high anodic stability. It was demonstrated that aluminium electrodes are fully passivated in solutions based on derivatives of pyrrolidinium with a $\text{N}(\text{SO}_2\text{CF}_3)_2^-$ anion and $\text{LiN}(\text{SO}_2\text{CF}_3)_2$.³⁵ Hence, in contrast to alkyl carbonate-based solutions in which $\text{LiN}(\text{SO}_2\text{CF}_3)_2$ has limited usefulness as a salt due to the poor passivation of aluminium in its solutions in the above IL-based systems, the use of $\text{N}(\text{SO}_2\text{CF}_3)_2^-$ as the anion doesn't limit their anodic stability at all. In fact it was possible to demonstrate prototype graphite/ $\text{LiMn}_{1.5}\text{Ni}_{0.5}\text{O}_4$ and $\text{Li}/\text{LiMn}_{1.5}\text{Ni}_{0.5}\text{O}_4$ cells operating even at 60 °C in solutions

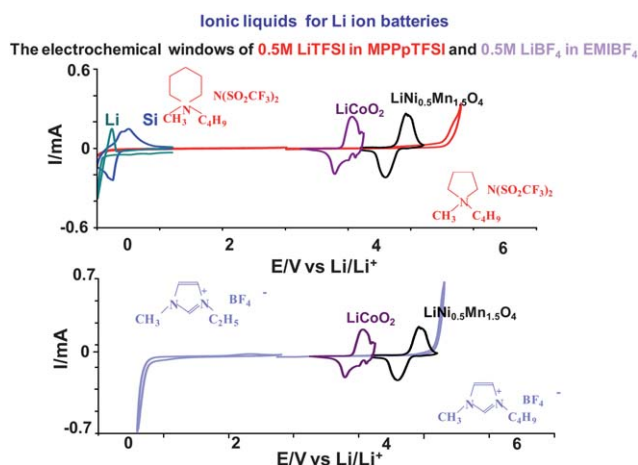


Fig. 3 Steady-state CV response of a Pt electrode in three IL solutions, as indicated. (See structure formulae presented therein.) The CV presentations include insets of steady-state CVs of four electrodes, as indicated: Li, Li–Si, LiCoO_2 , and $\text{LiMn}_{1.5}\text{Ni}_{0.5}\text{O}_4$.³⁴

comprising alkyl piperidinium- $\text{N}(\text{SO}_2\text{CF}_3)_2$ as the IL solvent and $\text{Li}(\text{SO}_2\text{CF}_3)_2$ as the electrolyte.³⁴

Challenges remain in as far as the use of these IL-based solutions with graphite electrodes.²² Fig. 4 shows the typical steady state of the CV of graphite electrodes in the IL without Li salts. The response in this graph reflects the reversible behavior of these electrodes which involves the insertion of the IL cations into the graphite lattice and their subsequent reduction at very low potentials. However when the IL contains Li salt, the nature of the reduction processes drastically changes. It was recently found that in the presence of Li ions the $\text{N}(\text{SO}_2\text{CF}_3)_2^-$ anion is reduced to insoluble ionic compounds such as LiF , LiCF_3 , LiSO_2CF_3 , $\text{Li}_2\text{S}_2\text{O}_4$ etc., which passivate graphite electrodes to different extents, depending on their morphology (Fig. 4).²² Fig. 4b shows a typical SEM image of a natural graphite (NG) particle with a schematic view of its edge planes. Fig. 4c shows the first CVs of composite electrodes comprising NG particles in the $\text{Li}(\text{SO}_2\text{CF}_3)_2/\text{IL}$ solution. These voltammograms reflect an irreversible cathodic wave at the first cycle that belongs to the reduction and passivation processes and their highly reversible repeated Li insertion into the electrodes comprising NG. Reversible capacities close to the theoretical ones have been measured. Fig. 4d and e reflect the structure and behavior of synthetic graphite flakes. The edge planes of these particles are assumed to be much rougher than those of the NG particles, and

so their passivation in the same IL solutions is not reached easily. Their voltammetric response reflects the co-insertion of the IL cations (peaks at 0.5 V vs. Li) together with Li insertion at the lower potentials (<0.3 V vs. Li). Passivation of this type of graphite is obtained gradually upon repeated cycling (Fig. 4e), and the steady-state capacity that can be obtained is much lower than the theoretical one (372 mA h g^{-1}).

Hence it seems that using graphite particles with suitable morphologies can enable their highly reversible and stable operation in cyclic ammonium-based ILs. This would make it possible to operate high voltage Li-ion batteries even at elevated temperatures (e.g. 4.7–4.8 V graphite/ $\text{LiMn}_{1.5}\text{Ni}_{0.5}\text{O}_4$ cells).³⁴ The main challenge in this field is to demonstrate the reasonable performance of cells with IL-based electrolytes at high rates and low temperatures. To this end, the use of different blends of ILs may lead to future breakthroughs.

Current collectors

The current collectors used in Li-ion systems for the cathodes can also affect the anodic stability of the electrolyte solutions. Many common metals will dissolve in aprotic solutions in the potential ranges used with advanced cathode materials (up to 5 V vs. Li). Inert metals such as Pt and Au are also irrelevant due to cost considerations. Aluminium, however, is both abundant and

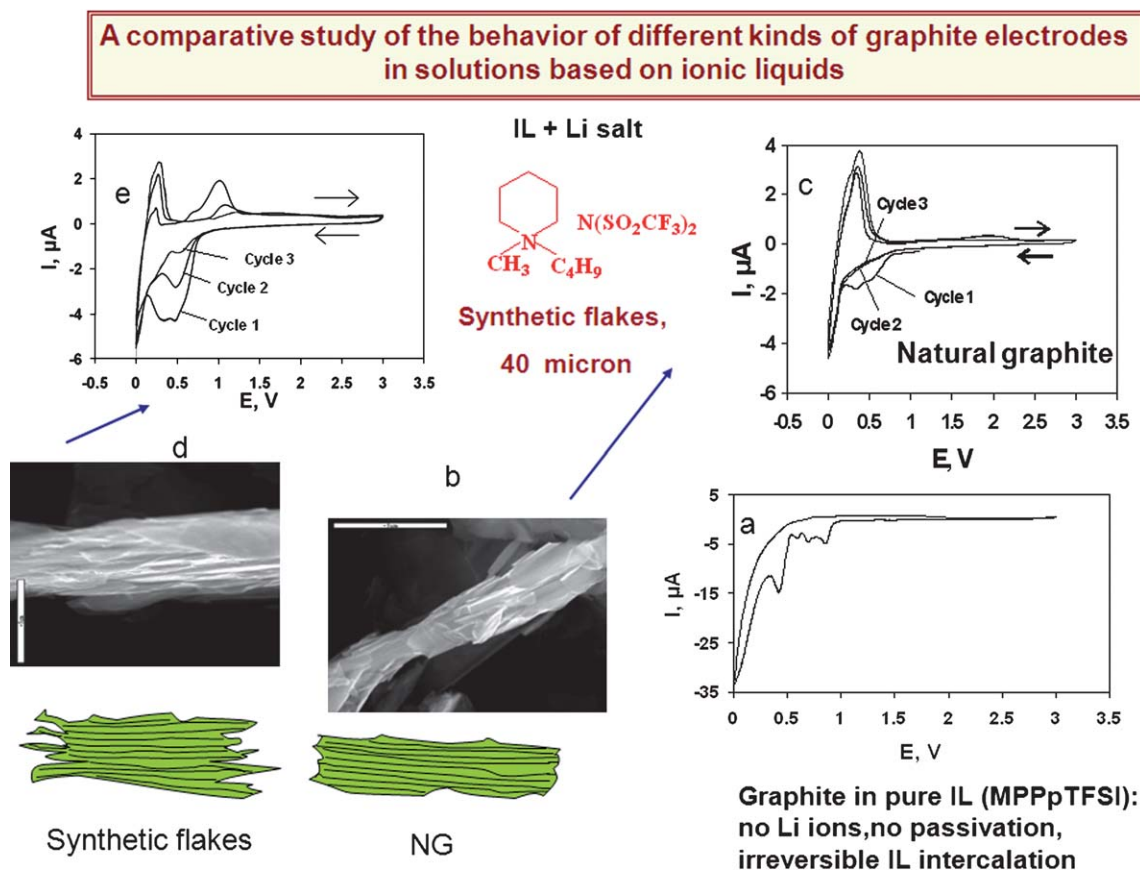


Fig. 4 A collection of data related to the behavior of graphite electrodes in butyl, methyl piperidinium IL solutions.²² (a) The behavior of natural graphite electrodes in pure IL without Li salt (steady-state CV is presented). (b) The schematic morphology and a SEM image of natural graphite (NG) flakes. (c) The CV response (3 first consecutive cycles) of NG electrodes in IL/0.5 lithium trifluoromethanesulfonimide (LiTFSI) solution. (d and e) Same as (b and c) but for synthetic graphite flakes.

cheap and functions very well as a current collector due to its excellent passivation properties which allow it a high anodic stability. The question remains as to what extent Al surfaces can maintain the stability required for advanced cathode materials (up to 5 V vs. Li), especially at elevated temperatures.

Fig. 5 presents the potentiodynamic response of Al electrodes in various EC–DMC solutions, considered the alkyl carbonate solvent mixture with the highest anodic stability, at 30 and 60 °C.³⁷ The inset to this picture shows several images in which it is demonstrated that Al surfaces are indeed active and develop unique morphologies in the various solutions due to their obvious anodic processes in solutions, some of which lead to their effective passivation. The electrolyte used has a critical impact on the anodic stability of the Al. In general, LiPF₆ solutions demonstrate the highest stability even at elevated temperatures due to the formation of surface AlF₃ and even Al(PF₆)₃. Al CCs in EC–DMC/LiPF₆ solutions provide the highest anodic stability possible for conventional electrode/solution systems. This was demonstrated for Li/LiMn_{1.5}Ni_{0.5}O₄ spinel (4.8 V) cells, even at 60 °C.³⁶ *This was also confirmed using bare Al electrodes polarized up to 5 V at 60 °C; the anodic currents were seen to decay to negligible values due to passivation, mostly by surface AlF₃.*³⁷ Passivation can also be reached in Li(SO₂CF₃), LiClO₄ and LiBOB solutions (Fig. 5). *Above 4 V (vs. Li), the formation of a successful passivation layer on Al CCs is highly dependent on the electrolyte formula used.* The anodic stability of EC–DMC/LiPF₆ solutions and Al current collectors may be further enhanced by the use of additives, but a review of additives in itself deserves an article of its own and for this readers are again referred to the review by Xu.³² *When discussing the topic of current collectors for Li ion battery electrodes, it is important to note the highly innovative work on (particularly anodic) current collectors by Taberna et al. on nano-architected Cu CCs⁴⁷ and Hu et al. who assembled CCs based on carbon nano-tubes for flexible paper-like batteries,³⁸ both of whom demonstrated superb rate capabilities.³⁹*

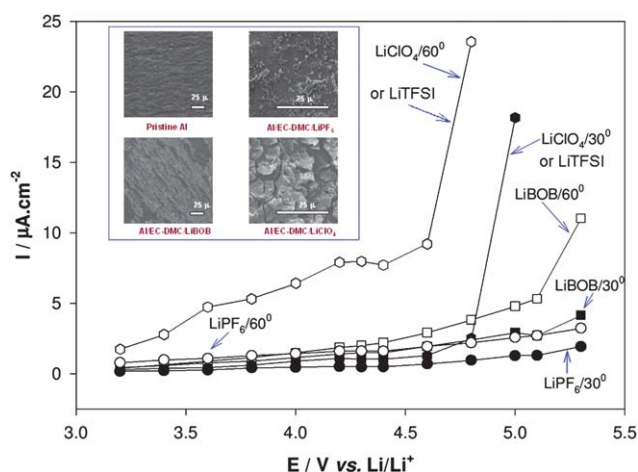
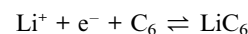


Fig. 5 The potentiodynamic behavior of Al electrodes (current density measured vs. E during linear potential scanning) in various solutions at 30 and 60 °C, as indicated. The inset shows SEM micrographs of passivated Al surfaces by the anodic polarization to 5 V in the solutions indicated therein.³⁷

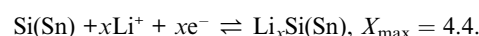
Anodes

The anode section in Fig. 1 indicates four of the most promising groups of materials whose Li-ion chemistry is elaborated as follows:

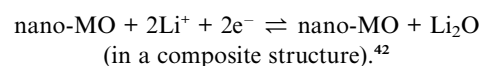
1. Carbonaceous materials/graphite:



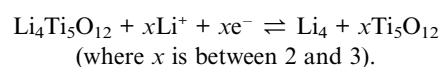
2. Sn and Si-based alloys and composites:^{40,41}



3. Metal oxides (*i.e.* conversion reactions):



4. Li_xTiO_y electrodes (most importantly, the Li₄Ti₅O₁₂ spinel structure).⁴³



Conversion reactions, while they demonstrate capacities much higher than that of graphite, are, practically speaking, not very well-suited for use as anodes in Li-ion batteries as they generally take place below the thermodynamic limit of most developed electrolyte solutions.⁴² In addition, as the reactions require a nanostructuring of the materials, their stability at elevated temperatures will necessarily be an issue because of the higher reactivity (due to the 1000-fold increase in surface area). As per the published research on this topic, only a limited meta-stability has been demonstrated. Practically speaking, it does not seem likely that Li batteries comprising nano-MO anodes will ever reach the prolonged cycle life and stability required for EV applications.

Tin and silicon behave similarly upon alloying with Li, with similar stoichiometries and >300% volume changes upon lithiation,⁴⁴ but the latter remain more popular, as Si is much more abundant than Sn, and Li–Si electrodes indicate a 4-fold higher capacity. The main approaches for attaining a workable reversibility in the Si(Sn)–Li alloying reactions have been through the use of both nanoparticles (*e.g.*, a Si–C nanocomposites⁴⁵) and composite structures (Si/Sn–M1–M2 inter-metallic compounds⁴⁴), both of which can better accommodate these huge volume changes. The type of binder used in composite electrodes containing Si particles is very important. Extensive work has been conducted to determine suitable binders for these systems that can improve the stability and cycle life of composite silicon electrodes.⁴⁶ As the practical usage of these systems for EV applications is far from maturity, these electrodes are not discussed in depth in this paper. However it is important to note that there have been several recent demonstrations of how silica wires and carpets of Si nano-rods can act as much improved anode materials for Li battery systems in that they can serve as

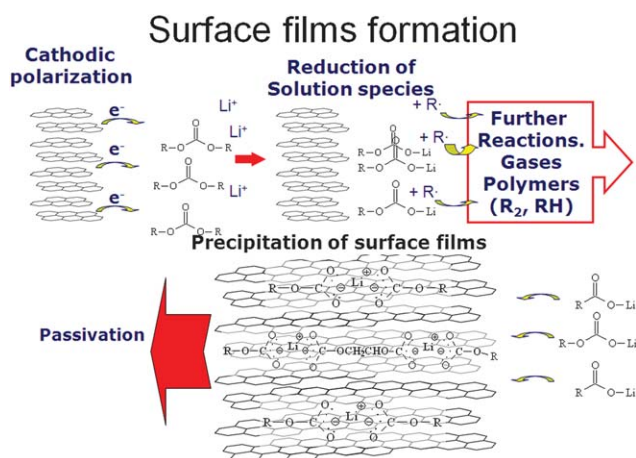


Fig. 6 A schematic presentation of the passivation formation on graphite electrodes, due to the reduction of alkyl carbonates and the precipitation of surface films comprising ROCO_2Li compounds in which the carbonate groups are bridged by Li ions.

stand alone, binder-free anodes, demonstrating more impressive cycle lives.⁴⁷

With a lithiation red-ox potential of ~ 1.5 V, almost within the thermodynamic stability limits of standard electrolyte solutions, $\text{Li}_4\text{Ti}_5\text{O}_{12}$, in the form of nanoparticles, demonstrates high stability (zero stress upon reversible lithiation), and very fast charge/discharge rates.⁴⁴ However, its limited capacity (~ 160 mA h g^{-1}) makes this material almost irrelevant for the high energy density batteries required for EV applications. Due to its other excellent properties, though, such as high rate capabilities, cycle life, stability, and safety features, this anode material may be important for other applications (e.g., load leveling and low temperature batteries—see later discussion). In addition, this anode material can serve as an important probe counter electrode (anode) for studies aimed at exploring the intrinsic behavior of cathode materials without interference and reflection from the anode side (as is the case for cells comprising graphite or other low potential anodes). *It is important to note also that LTO anode materials can be further improved by doping, especially in order to increase their electronic conductivity, hence augmenting their potential future use as a fast electrode material.*⁴⁸

It is generally accepted by the battery community, including the authors of this article, that graphite electrodes will remain the most important and relevant anodes in Li-ion batteries for EV application for some time to come, therefore these electrodes deserve special discussion. An interesting feature of Li graphite electrodes is their stability despite their fragile structure, and the fact that their red-ox activity with Li ions, approximately 0.25–0.05 V vs. Li, is well below the cathodic stability limit of all the relevant electrolyte solutions. Li graphite electrodes are naturally passivated in alkyl carbonate solutions; their reversible behavior and stability in fact depend solely on these passivation phenomena.²⁷ The surface chemistry of graphite electrodes has been thoroughly explored.³⁰ Fig. 2 indicates the typical potentiodynamic behavior of Li salt solutions in several families of polar aprotic solvents cycled against inert Pt electrodes and Scheme 1 describes the main reactions of EC at low potentials.^{26,31} As the anodic stability of solvents is augmented due to

the presence of functional groups with high oxidation states, so their cathodic stability is necessarily lower (more easily prone to reduction). However the reduction of trace O_2 (<2 V vs. Li), H_2O (~ 1.5 V vs. Li), and solvents such as alkyl carbonate (<1.5 V vs. Li) in the presence of Li ions leads to the precipitation of insoluble ionic Li compounds: Li_2O , LiOH , Li_2CO_3 , ROCO_2Li , etc., the nature of which depend highly on the electrolyte salt used. These products form surface layers that comprise the SEI.²⁶

Fig. 6 illustrates one of the main scenarios of the passivation process of graphite: when graphite electrodes are polarized to potentials below 1.5 V (vs. Li) in alkyl carbonate solutions, solvent reduction occurs and the charge transfer forms Li-ion-stabilized radical anions which in turn decompose to ROCO_2Li and alkyl-containing moieties as suggested by spectroscopic studies in ref. 27–31 and 46–50 (see Fig. 2). These products may either precipitate on the electrodes as surface films, or continue to react even further in the solution phase. The FTIR spectra of the surface films formed on Li, Li-graphite and Li-Si electrodes in alkyl carbonate solutions that are not contaminated by acidic species reflect the formation of dimers and trimers of carbonate moieties in which Li ions bridge between carbonate groups, and between the carbonate groups and the negatively charged electrode surfaces.⁴⁹ These interactions lead to a reasonable adhesion and cohesion of the surface species which form stable, passivating surface films. The ionic structure of these films (carbonate groups linked by Li ions) leads to their very good Li-ion mobility, and as they reach a certain thickness, further electron transfer is diminished. Thus, the electrodes reach meta-stability. In LiPF_6 solutions, surface alkoxide species such as $\text{LiOCH}_2\text{CH}_2\text{OLi}$ precipitate to form Li-ion conducting, passivating surface films.^{29,30} The main problem with the stability of Li-intercalated graphite electrodes is the fact that this material is quite fragile, making it vulnerable to cracking and exfoliation. There are two main detrimental scenarios related to graphite electrodes: co-intercalation into or between the particles, and the subsequent reduction of those species. Co-intercalation with the Li ions of the solvent molecules into graphite may occur at potentials higher than those of Li intercalation, *i.e.* before full surface passivation takes place. This insertion process of large solvated ions may be enough to cause exfoliation. Upon further cathodic polarization it is likely that the inserted solvent molecules are subsequently reduced to form ionic compounds and gases that have the potential to seriously damage the graphite particles.⁵⁰ Even in the absence of true solvent co-intercalation phenomena, the edge planes of graphite particles contain many crevices. The reduction of the solution species inside such crevices can also create internal pressures, which can lead to a cracking of the particles.^{51,52} Fig. 7 details these detrimental scenarios. This same figure also shows *in situ* AFM images of cathodically polarized graphite in which the formation of a crack was imaged. After the initial cracking, the freshly cleaved surface was exposed to the solution and reacted with additional solution species, which finally partially filled the crack with solid reduction products.⁵² When the first process is sufficiently fast, the reduction products quickly form passivating surface films that hinder excessive electron transfer to solution species, preventing the detrimental reduction of solution species within the graphite particles. If the solution reduction products cannot form the protecting surface films quickly enough, then there is enough time for the

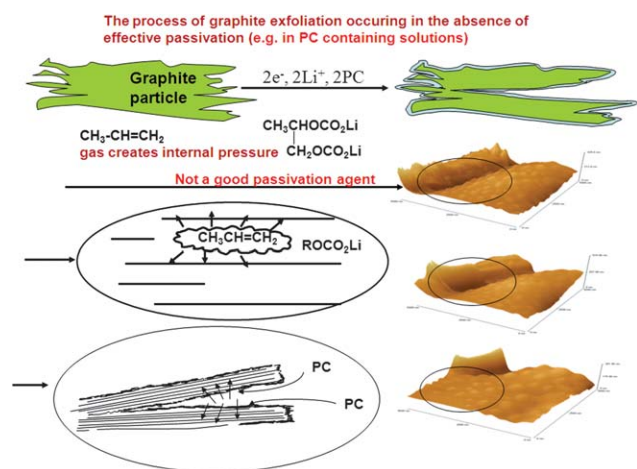


Fig. 7 A schematic presentation of possible cracking of graphite electrodes due to the reduction of solution species within the graphite particles, and AFM images of a graphite surface measured *in situ* in which cracking was observed (EC-PC/LiClO₄ solution^{51,52}).

co-intercalation of solvent molecules and the consequent detrimental reduction processes within the particles.

This phenomenon can have potentially significant implications. For instance in the case of ethylene *versus* propylene carbonate (EC *vs.* PC), common electrolyte solvents which differ by only a methyl group and exhibit similar reduction processes (e.g. the main products are Li alkylene di-carbonates or alkoxides and alkylene gas), nevertheless, have pronouncedly different effects on the behavior of graphite electrodes in their presence. In EC-containing systems (e.g., EC + dimethyl carbonate, DMC), graphite electrodes are well-passivated and intercalate Li ions reversibly, while in PC-based solutions the electrodes exfoliate and do not demonstrate reversible insertion. One accepted explanation for the difference is that the methyl group in the reduction products of PC (e.g., CH₃CH(OCO₂Li)CH₂OCO₂Li or CH₃CH(OLi)CH₂OLi) may interfere with a fast formation of ordered surface films, while the reduction products of EC that contain only the –CH₂CH₂– group may form ordered surface films more quickly.

Even in the best solutions, graphite electrodes can never develop unlimited meta-stability. The known volume change of ~10% upon Li insertion/deinsertion during prolonged cycling, especially at elevated temperatures (e.g. 60 °C) causes the surface films to stress and crack, thereby limiting their infinitely stable passivation. Furthermore, upon very prolonged cycling graphite electrodes develop increasing impedance as their working potential must maintain a continuous driving force for further surface reactions. This means the gradual thickening of the surface films and an increase in the electrode's impedance.⁵³ However even in light of these limitations, graphite electrodes of the right morphology and surface chemistry considerations may still demonstrate sufficiently prolonged cycle lives, making them the suitable choice for EV applications.

Advanced cathode materials

It is difficult to say with certainty exactly which cathode materials are the most promising for EV applications, particularly with the consideration that they be developed within a realistic

time framework (a few years and less). However certain classes of materials show significant promise. The frontier of this research includes five main materials: Li–S, Li–air, LiMPO₄ (M = Mn, Fe, Co), Li₂MnO₃·Li[MnNiCo]O₂ and LiMn_{1.5}Ni_{0.5}O₄.

Li–S batteries have been studied by several groups, as well as ours^{54,55} but will not be discussed in depth here, as it is generally found so far that the life span that can be obtained with the most successful Li–S batteries (a few dozen cycles),⁵⁶ is nowhere near what is needed for EV applications. However these limits too may be superseded someday, as recent developments, for example, of cathodes in which sulfur is encapsulated in hollow carbon fibers,⁵⁷ or in which Li₂S functions as the starting pristine cathode material instead of elementary sulfur⁵⁸ appear to be leading to the possible development of stable sulfur cathodes that can undergo prolonged cycling. Another relatively novel system not discussed here is that of Li–air batteries, which are in a very basic and preliminary stage of research.⁵⁹ There are intrinsic problems of reversibility and compatibility in these systems, as well as great challenges in electrocatalysis at the air (cathode) side.^{60,61}

To date, the three remaining categories of materials show the best prospects for practical development. Studies being conducted in our lab involve materials from each of the three categories; *i.e.* Li[MnFe]PO₄, Li₂MnO₃·Li[MnNiCo]O₂, and LiMn_{1.5}Ni_{0.5}O₄. The successful practical implementation of any of these compounds as cathode materials could take Li-ion technology well beyond its current limits.

A lot of work has been devoted by this group as well as many others throughout the world to the LiMn_{1.5}Ni_{0.5}O₄ spinel which has a redox potential of approximately 4.7–4.8 V due to interactions of the Ni ions in the lattice ($Ni^{2+} + e^- \rightleftharpoons Ni^{3+}$; $Ni^{3+} + e^- \rightleftharpoons Ni^{2+}$).^{62,63} Despite the high voltage, we demonstrated Li/LiMn_{1.5}Ni_{0.5}O₄ cells on Al CC exhibiting prolonged cycling at 60 °C in EC–DMC/LiPF₆. A stable capacity was also demonstrated, even after prolonged aging at 70 °C.⁶⁴ The synthetic method used in the creation of this material and the morphology of the product both play an important role in its performance, whose theoretical capacity is approximately 145 mA h g⁻¹. Most publications demonstrate a capacity of less than 135 mA h g⁻¹, though it has been demonstrated through the use of the spinel structure to reach greater than 140 mA h g⁻¹ at high rates.⁶⁵ A review of the literature indicates that the best performance is obtained with micrometric-sized particles whose facets are very smooth.^{62–64} *The morphology of this cathode material is critical for its performance in connection to its surface chemistry: as the crystals are smoother, the surface reactions of Li_xMn_{1.5}Ni_{0.5}O₄ with solution species are more moderate. Overly intensive surface reactions of this material in solution lead to detrimental passivation phenomena.* Li_xMn_{1.5}Ni_{0.5}O₄ spinel has been shown to be fully compatible with standard electrolyte solutions (EC–DMC/LiPF₆),⁶⁵ hence the successful operation of the cells comprising this cathode material and low potential anodes such as Li or Li-graphite depend not on the intrinsic limitation of the cathode, but rather mostly on peripheral aspects (e.g. reflective relationship between the anode and that cathode, and the passivation of the negative electrodes).

The subset of Li-rich layered TMOs of the (Li₂MnO₃)_x(LiMO₂)_y type were discovered and developed by groups at the Argonne National Laboratory in the US.^{66,67} These

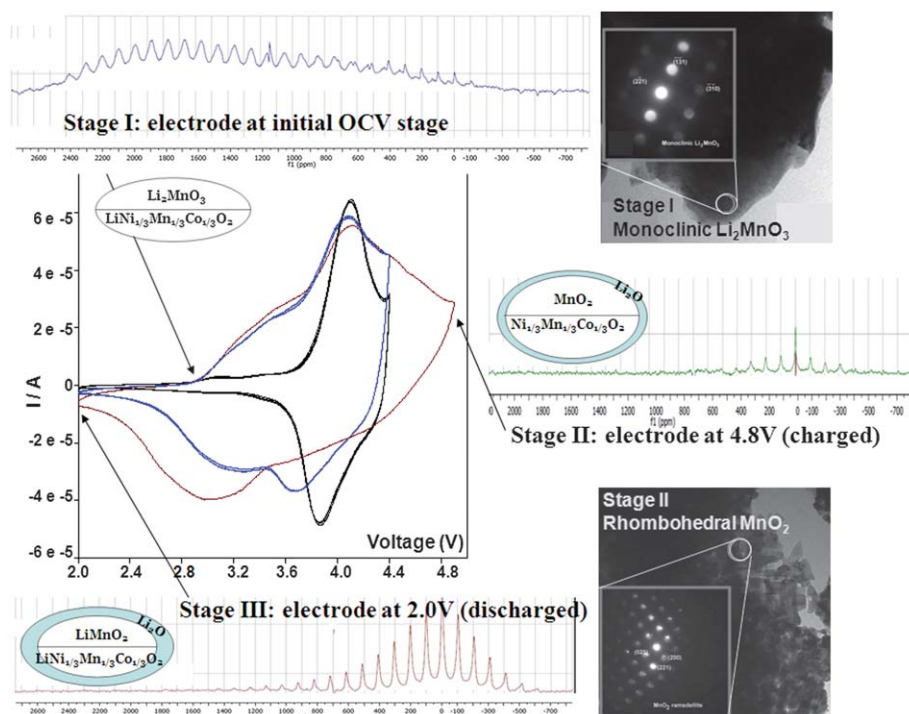


Fig. 8 Presentation of the behavior of $\text{Li}_2\text{MnO}_3 \cdot \text{LiMn}_{1/3}\text{Ni}_{1/3}\text{Co}_{1/3}\text{O}_2$ cathode material synthesized by SCR.⁶⁸ Typical CVs before and after activation, a typical HRTEM image of the pristine material and the activated material at delithiated and fully lithiated states (as indicated).

materials can reach capacities greater than 250 mA h g^{-1} and continue to be extensively studied. Data collected by this group involved $x\text{Li}_2\text{MnO}_3 \cdot (1-x)\text{LiMn}_{1/3}\text{Ni}_{1/3}\text{Co}_{1/3}\text{O}_2$, where, $x = 0.3, 0.5$ and 0.7 .⁶⁸ When the appropriate ratios of the transition metal cations in the synthesis mixture are used,

the SCR procedure, followed by calcination at 900°C , produces composite structures with the desired stoichiometries containing the monoclinic and rhombohedral phases (Li_2MnO_3 and $\text{Li}[\text{MnNiCo}]_2\text{O}_2$) at a variety of ratios, and well-mixed on the nano-metric level.

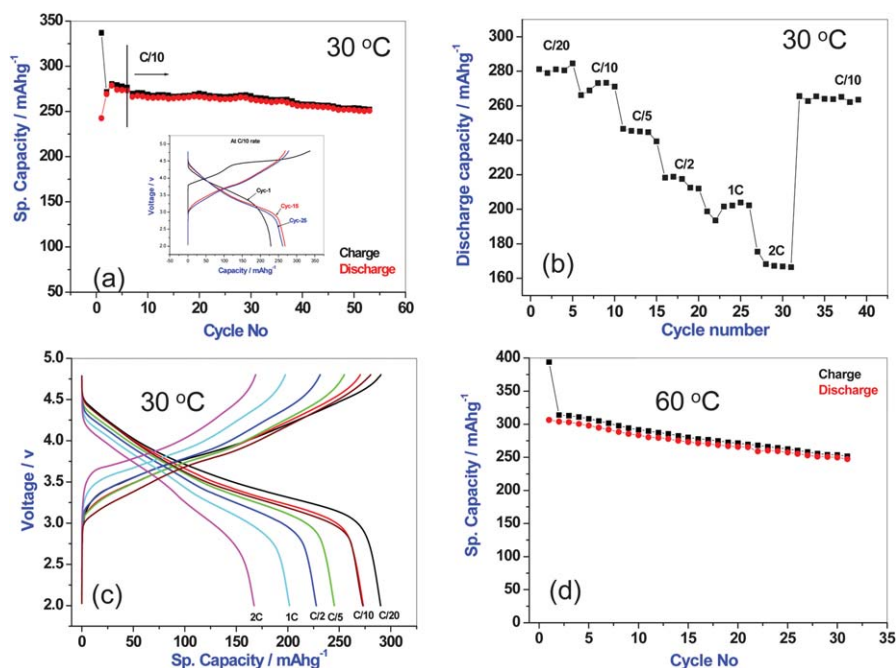


Fig. 9 A collection of electrochemical data related to activated $\text{Li}_2\text{MnO}_3 \cdot \text{Li}[\text{MnNiCo}]_2\text{O}_2$ electrodes: cycling data, rate capability tests (cycling at different rates), and voltage profiles at different rates in galvanostatic measurements, as indicated.

Fig. 8 and 9 show representative data on $0.5\text{Li}_2\text{MnO}_3 \cdot 0.5\text{LiMn}_{1/3}\text{Ni}_{1/3}\text{Co}_{1/3}\text{O}_2$ cathode material; this particular ratio of components was found to have the most promising stoichiometry and structure among the various combinations that were examined.⁶⁸ Fig. 8 indicates schematically the concept of these composite cathode materials. The atomic layering, elucidated by the XRD (not shown; refer to original paper, ref. 67) and electron diffraction (SAED) measurements, together with rigorous imaging by HRTEM, show unambiguously the coexistence of the two phases and their mixing at the molecular (nano) level. ^7Li SS NMR spectra of the pristine material suggest Li in at least two sites in the bulk, as marked in Fig. 8. In the 3–4.4 V cycling range, the CV exhibits a typical electrochemical behavior of the $\text{LiMn}_{1/3}\text{Ni}_{1/3}\text{Co}_{1/3}\text{O}_2$ material with a specific capacity around 80 mA h g^{-1} , expected for a material containing only 50% active mass (whose specific capacity is $160\text{--}170 \text{ mA h g}^{-1}$). Polarizing these electrodes to 4.9 V, however, activates the active mass and completely changes their structure, a phenomenon that is clearly indicated in the ^7Li NMR spectra (Fig. 8). This is reflected in the CV as well, which also shows the change in the electrochemical behavior as a result of this activation. The resulting increase in the specific capacity is remarkable; the activated material demonstrates extended redox behavior in the 2–4.5 V range with reversible capacity around 250 mA h g^{-1} , and a voltammetric response which appears to reflect the lithiation–delithiation processes suggestive of the formation of a solid solution.

Fig. 9 shows the results of typical voltage profiles of prolonged galvanostatic cycling (Fig. 9a) and rate capability tests (Fig. 9b and c) at 30°C . Our studies show that these electrodes can produce capacities higher than 200 mA h g^{-1} during prolonged cycling at 60°C (Fig. 9d) in standard electrolyte solutions. Cycling at elevated temperatures not only does not impede, but even stabilizes their cycling behavior. It is clear from our studies that the structure of these composite materials before and after activation is complicated and fragile. Their activation, which involves the loss of oxygen from the bulk, forms a high capacity, layered active Li_xMO_y material that includes a Li_2O surface layer, suggested by the ^7Li NMR and HRTEM data. Since these materials are electroactive within a wide voltage range, it is impossible to determine a specific representative voltage, but rather only a mean. Following these average voltages during cycling often reveals gradual changes, which suggest continuous structural changes in the material. The challenges remaining for these materials include: stabilization during prolonged cycling, improving their rate capabilities, and demonstrating acceptable safety features. The best approaches seem to be to address both their synthetic processes and the use of coatings. For example it was found that coating Li_xMO_y cathode materials with thin layers of Al_2O_3 , AlPO_4 and MgO can increase their stabilities.^{69–71} An additional approach is the consideration of different electrolyte materials. Since these compounds are considered high voltage systems, it remains unclear whether the currently used standard electrolyte solutions are the most appropriate for their use. Though much work needs to be done towards addressing these issues, these materials could still be considered the most promising cathode materials available to date. One of the main strategies to improve the rate capability and safety of Li_xMO_y cathode materials is to develop powders with

core–shell structures: active mass particles coated with protective layers that reduce detrimental reactions of the cathode material with solution species, yet allow fast migration of Li ions through them. Successful surface coatings make possible the use of nanoparticles in composite cathodes (with the core–shell structure). If the surface reactivity of nano-particles can be properly attenuated, this can significantly increase the rate capabilities obtainable with practical composite cathodes. Though the use of nano-particles in composite electrodes may create serious problems in terms of mechanical and electronic integrity of the active mass, effective methods have been reported that address these issues and can thus enhance the integrity of such composite electrodes.⁷²

The last of the cathode materials dealt with in this review is the olivine LiMPO_4 family, where M can be Fe, Mn, Co, and Ni, exhibiting the following redox potentials: 3.5, 4.1, 4.8 and 5.2 V vs. Li, respectively. In order to facilitate their kinetics as Li-insertion electrodes, as these compounds are intrinsically slow in both electrons and Li-ion transport,⁷³ their successful usage has been due to their assembly in nanoscale particles. Due to its restrictively high redox potential, LiNiPO_4 is not realistically considered as a relevant cathode material. LiCoPO_4 is considered to be more relevant as its redox activity is less than 5 V, therefore falling within the electrochemical window of standard electrolyte solutions. Our work with this material indicates that extensive efforts are still needed in order to develop a reliable synthesis for LiCoPO_4 as well as to match it with electrolyte systems in which it can operate stably. LiFePO_4 was introduced as a cathode material 13 years ago by Goodenough *et al.*⁷³ Since then, extensive work has been devoted to this material, which has since been brought to a practical level of commercial usage. Companies such as Sud-Chemie produce LiFePO_4 that reaches a capacity of approximately 165 mA h g^{-1} and demonstrates excellent rate cyclability and safety features.⁷⁴ Many of these features, including its excellent low temperature performance, could make it a promising cathode material for EV applications as well.^{75,76} However its redox potential of $\sim 3.5 \text{ V}$ vs. Li means that Li-ion batteries using this cathode material vs. graphite can reach a potential of only 3.4 V, therefore modules for EV comprising graphite/ LiFePO_4 cells would possess energy densities below 100 W h kg^{-1} .⁷⁷ This level of battery performance

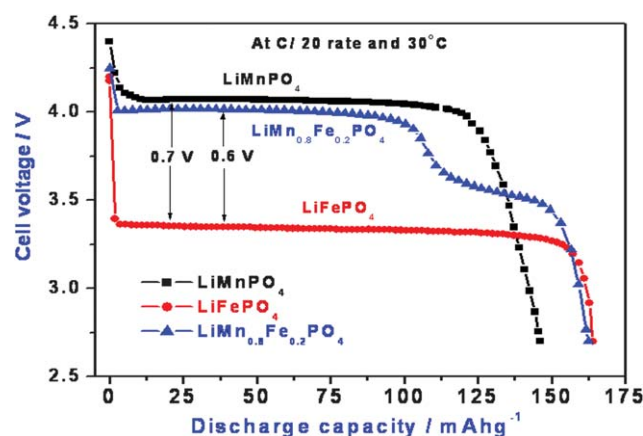


Fig. 10 Voltage profiles of Li_xFePO_4 , Li_xMnPO_4 and $\text{Li}_x\text{Mn}_{0.8}\text{Fe}_{0.2}\text{PO}_4$ electrodes measured during galvanostatic discharge (lithiation) in EC-DMC/1 M LiPF_6 1 M at C/10 rates.^{79,80}

would enable a full EV to drive no more than 150 km at reasonable speeds (e.g. around 100 km h⁻¹) between charges.⁷⁸ With the successes of LiFePO₄ in mind, researchers in this field have turned their attentions to its Mn-containing analog, LiMnPO₄, as the theoretical voltage potential of this material is 600 mV higher. Fig. 10 compares the voltage profiles of LiFePO₄, LiMnPO₄ and LiMn_{0.8}Fe_{0.2}PO₄ electrodes and reflects both the benefits and shortcomings of the Mn-based olivine cathodes.^{78,79} The practical challenge remains to obtain similar performance metrics for this material, as this breakthrough would significantly increase the usable energy densities of Li-ion batteries with LiMPO₄ cathodes.

It is important to note that since the oxygen atoms in LiMPO₄ are much less basic and nucleophilic than those of Li_xMO_y compounds, the Li-olivine compounds are much less reactive with solution species than Li_xMO_y compounds.^{78,79} This fact is critical to their functionability as nano-materials. That is, the decrease in Li-ion diffusion pathways in the smaller particles is not offset by the typically noted associated increase in surface film formation due to the huge increase in surface area. *The application of a thin carbon coating on the nano-LiMPO₄ particles further facilitates electron transport as it enables better interparticle electrical contact. In fact, the use of thin carbon coating is a critical component for LiMPO₄ species and is mandatory for their operation as fast cathode materials, due to the poor intrinsic transport properties of these powders. The carbon coating increases the rate capability of many of the LiMPO₄ cathode materials by several orders of magnitude.* Fig. 10 shows the best voltage profiles obtained for LiFePO₄ and LiMnPO₄. While LiFePO₄ electrodes can nearly reach their theoretical capacity (170 mA g⁻¹) in repeated Li-ion insertion/deinsertion cycling, the state-of-the-art LiMnPO₄ can reach no more than 90% of its theoretical capacity (up to 150 mA h g⁻¹). LiMnPO₄ was studied intensively by this group and could be considered the best choice of the olivines according to its demonstrated capacities and rate capabilities.⁷⁹ Its redox potential of ~4.1 V vs. Li is well within the anodic stability limits of aluminium current collectors and alkyl carbonates (e.g., EC–DMC)/LiPF₆ solutions. Composite LiMnPO₄/C electrodes can reach 100% cycling efficiencies, demonstrating a capacity of 150 mA h g⁻¹ in very prolonged cycling experiments. Hundreds of cycles were performed at 60 °C, even in coin-type cells. The surface reactivity of this material was found to be as low as that of LiFePO₄, and therefore it was possible to use it as nanoparticles and obtain even better rate capabilities than that of LiNi_{0.5}Mn_{0.5}O₂ and LiNi_{0.8}Co_{0.15}Al_{0.05}O₂ (both of which are important due to their high practical specific capacities which exceed 180 mA h g⁻¹). However LiMnPO₄ remains inferior to LiFePO₄ in terms of both capacity and rate capability. To date, the reason for that is not clear. As demonstrated in Fig. 10, a replacement of 20% Mn by Fe in LiMnPO₄, thus forming a LiMn_{0.8}Fe_{0.2}PO₄ compound, demonstrates the properties of a highly interesting and important cathode material whose practical capacity (165 mA g⁻¹) is close to the theoretical one, similar to that of the state-of-the-art LiFePO₄ material.⁸⁰ This compound is in fact a true solid solution of LiMnPO₄ and LiFePO₄, as demonstrated by its voltage profile, which nicely reflects the red-ox reaction of both Mn^{2+/3+} and Fe^{2+/3+} with the expected proportional contributions. As seen in Fig. 10, the solid solution leads to the combined influence of

the two redox centers (the red-ox voltage of the Mn^{2+/3+} is slightly lower, and that of Fe^{2+/3+} is significantly higher in Li[MnFe]PO₄ compared to the mother LiMPO₄ compounds). Fig. 11 provides a collection of data from intensive work with LiMn_{0.8}Fe_{0.2}O₄ electrodes. Raman, Mössbauer and HR-TEM measurements of carbon-coated nanoparticles after prolonged aging in standard solutions at elevated temperatures confirmed the excellent stability of this active mass (see Fig. 11a–c). FTIR and XPS measurements of aged and cycled material (not presented in this review) clearly indicate that its surface stability is much greater than that of Li_xMO_y compounds.⁸⁰ The main phenomenon detected after prolonged aging in LiPF₆ solutions was the formation of surface LiF. The most important results were its very high stability, which enabled the demonstration of the very prolonged cycling of Li/LiMn_{0.8}Fe_{0.2}PO₄ cells at elevated temperatures, and its excellent rate capabilities. Fig. 11d and e display the results of comparative experiments in which coin-type cells containing different cathodes vs. Li metal anodes in EC–DMC/LiPF₆ solution were cycled at different rates, as indicated. Cathode capacity and energy density are seen to be functions of the rates used. The energy density was calculated by integrating the capacity and voltage of the electrodes during discharge (lithiation). The superior rate capability of LiMn_{0.8}Fe_{0.2}PO₄ electrodes is clear from these charts and related experiments. Therefore Li[MnFe]PO₄ can be considered a practically important novel cathode material for Li-ion batteries. Finally, despite a recent publication on the apparent thermal instability of delithiated Li_xMnPO₄,⁸¹ our thermal studies show that LiFePO₄, LiMnPO₄ and Li[MnFe]PO₄ demonstrate very similar good thermal behavior in contact with standard electrolyte solutions in both fully lithiated and delithiated states. The three compounds are much more thermally stable than Li_xMO₂ cathode materials in both spinel and layered structures.

Temperature-related performance

Most commonly used electrodes can function well at elevated temperatures (e.g. 60 °C in standard electrolyte solutions). Their stability at elevated temperature can be enhanced by the use of additives.³² The good performance of many electrodes at low temperatures remains a bigger challenge. Therefore the focus here will be on low temperature studies.

In terms of the electrolytes, neither the above-discussed IL-based electrolyte systems nor EC–DMC/LiPF₆ solutions succeed at low temperatures. The latter solutions, which demonstrate so many advantages in terms of high anodic stability and excellent passivation of low-potential anodes, cannot function below –15 to –20 °C, as their conductivity drops drastically due to the solidification of EC and the reduced solubility of the Li salt. In order to obtain solutions that can work at very low temperatures (with a reasonable criterion: ionic conductivity greater than 1 mS cm⁻¹ at 40 °C), it is necessary to add additional solvent components to the binary EC–DMC solutions. A lot of work has been devoted to solutions of Li salts in ternary and quaternary solvent mixtures that demonstrate reasonable ionic conductivities at low temperatures.⁸² However, more components result in lower anodic stability and more complicated electrode surface chemistry. This latter effect may lead to poor anodic passivation. We found that adding ethyl

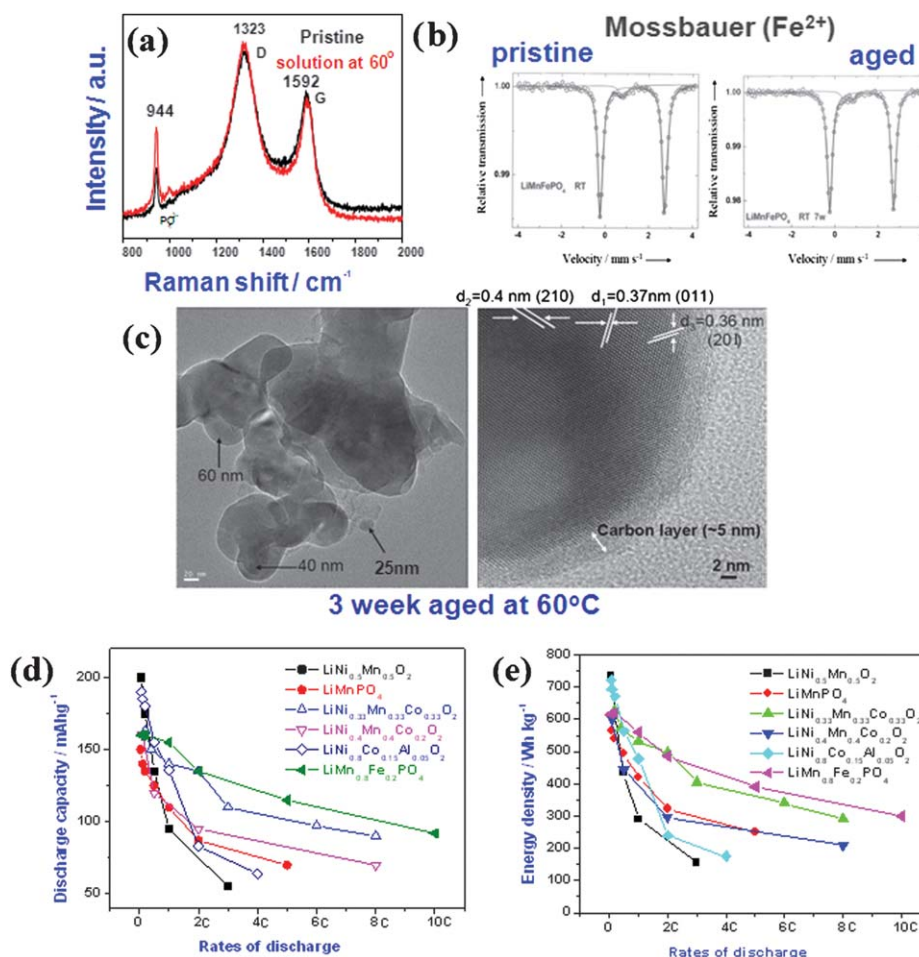


Fig. 11 A collection of data related to $\text{LiMn}_{0.8}\text{Fe}_{0.2}\text{O}_4$ electrodes.⁸¹ (a) Raman spectra of pristine and aged particles. (b) Fe Mössbauer spectra of pristine and aged material. (c) HRTEM of aged particles. Aging was carried out at 60 °C in an EC–DMC/LiPF₆ 1 M solution. (d) Capacity vs. rates of various cathodes, as indicated, in galvanostatic measurements, 30 °C, EC–DMC/LiPF₆ 1 M solutions. (e) Energy density vs. rates of various cathodes (indicated) in the same experiments (related to (d)). The energy density was calculated from the voltage profiles by integrating capacity over voltage.

methyl carbonate (EMC) as a fourth component to EC–DMC/LiPF₆ solutions is enough to reach a reasonable conductivity at –40 °C.⁸³ The benefit is that the addition of EMC still does not drastically change the surface chemistry and therefore does not effect the very good passivation properties of electrodes in EC–DMC-based solution alone. VC can be added as an additive to enhance the passivation of both graphite anodes and Li_xMO_y (lithiated transition metal oxide (TMO)) cathodes.

For the most part, electrode performance also declines at low temperatures. Fig. 12 presents the conductivity/temperature relationship of an EC–DMC–EMC/LiPF₆ solution with an optimized composition and the steady-state capacity of various electrodes measured in this solution at low rates ($C/20$ – $C/10$). As demonstrated, the low temperature performance of both graphite electrodes and lithiated TMO cathodes ($\text{Li}(\text{MnNiCo})\text{O}_2$, $\text{Li}[\text{NiCoAl}]\text{O}_2$) is poor. As demonstrated in this figure for graphite electrodes, the electrode's surface area also plays a role in the low temperature performance of Li insertion electrodes. A higher specific surface area (~ 7 vs. $0.5 \text{ m}^2 \text{ g}^{-1}$) leads to higher capacity at low temperatures, though this relationship is not linearly proportional.

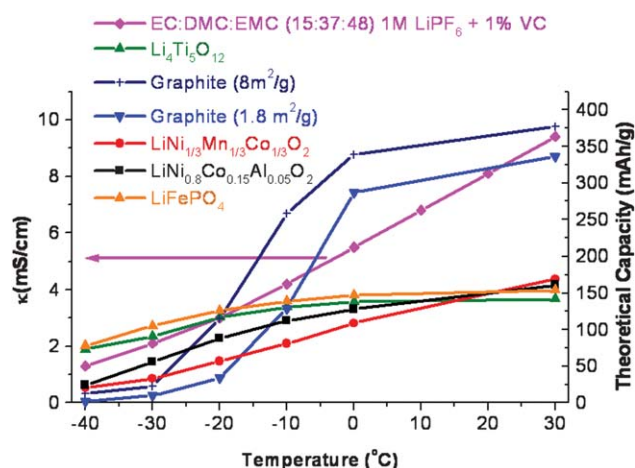


Fig. 12 The ionic conductivity/temperature dependence of EC–DMC–EMC (15 : 37 : 48 by weight)/LiPF₆ 1 M + 1% (by weight) VC, and the steady-state capacity of various electrodes (indicated) as a function of temperature, upon galvanostatic cycling in the same solution at $C/20$ rates.⁸³

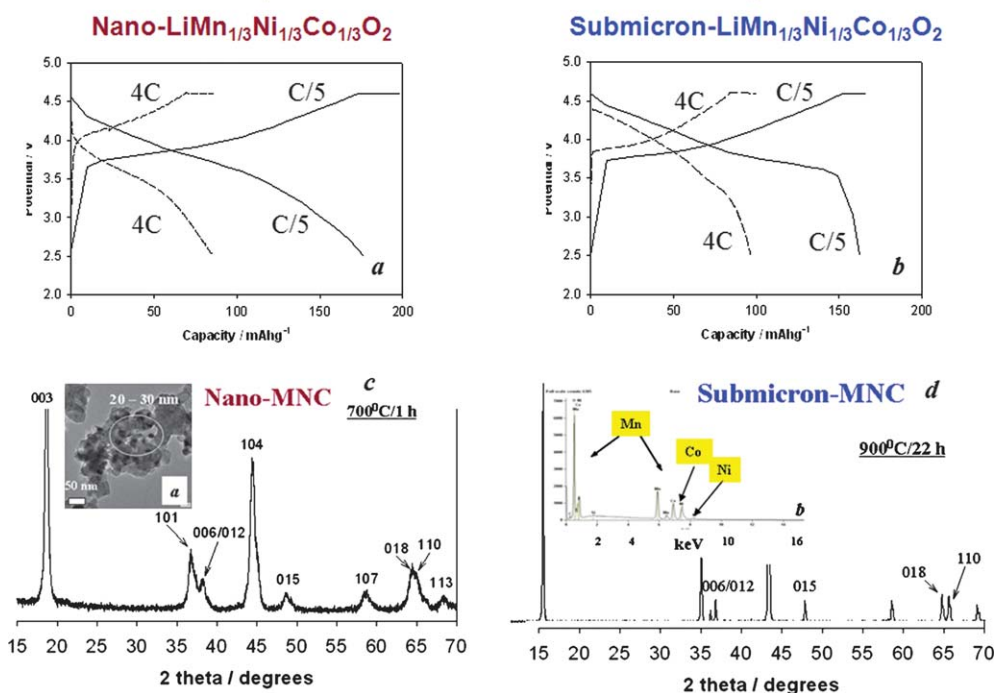
Electrolyte solution: EC-DMC/1M LiPF₆

Fig. 13 XRD patterns (c and d) of nano- and submicrometric size $\text{LiMn}_{1/3}\text{Ni}_{1/3}\text{Co}_{1/3}\text{O}_2$ particles synthesized by SCR and further calcinations in air (700 °C/1h and 900 °C/22 h, respectively), and voltage profiles of electrodes comprising these materials measured at two different rates, as indicated (galvanostatic measurements in EC-DMC/LiPF₆ 1 M solutions (a and b)). The insets show a SEM micrograph of the nanoparticles and element analysis by EDS.⁸⁴

The electrode materials that demonstrate the most success under these conditions are $\text{Li}_4\text{Ti}_5\text{O}_{12}$ and LiFePO_4 nanoparticles. As demonstrated in Fig. 12, they both demonstrate reasonably good low temperature performance.⁸³ Of all known cathode materials, Li_xTiO_y and LiMPO_4 ($\text{M} = \text{Fe, Mn}$ or both) are among the few that can be used as nanoparticles at all, and thus benefiting from the greatly shortened Li-diffusion lengths which correspond to their achieving very fast cycling rates. This functionality at the nanoscale is in fact because both families of materials have a relatively low surface reactivity in standard electrolyte solutions. The LTO materials red-ox potential is sufficiently high, above the thermodynamic cathodic stability of alkyl carbonate solutions (<1.5 V vs. Li). The red-ox potential of LiFePO_4 and LiMn_2O_4 (3.5 and 4.1 V vs. Li, respectively) are below the onset of the oxidation of alkyl carbonates. However, what is more important is that the oxygen atoms in the olivine compounds, bound to P^{5+} ions, are much less nucleophilic and basic compared to the oxygen atoms of Li_xMO_y (lithiated TMO). This cycling capability at the nanoscale makes these materials unique in their superb performance even at low temperatures.

On the use of nanoparticles

In the field of material science there is a general trend to introduce nanomaterials to take advantage of their unique qualities. In the past few years these forays have extended into the Li battery field. The use of nanoscaled compounds as intercalation materials have the obvious advantage of greatly decreased lithium ion diffusion lengths and more highly facilitated

interfacial charge transfers due to the associated increase in surface area. However due to the fact that in most Li-ion battery systems neither anode nor cathode ever attain complete thermodynamic equilibrium while in contact with relevant electrolyte solutions, so that the increases in surface areas then have the effect of associated increases in surface reactivity, which in most cases leads to an enhancement of side reactions between the electrodes and the electrolyte, leading to a destabilization of the active material as well as an increase in impeding passivation phenomena. An example is given below.

The work done in this lab involved a SCR synthesis using relevant metal nitrates (oxidizing agents) in aqueous media with sucrose as fuel, varying the stoichiometry of the compounds. These syntheses produce nanoparticles which can be subject to further sintering to sub-micrometric and micronic-size particles, the duration of which determines the average particle size.²⁴ Hence, it was possible to compare both nano- and sub-micronic size particles of different cathode materials synthesized from the same batch of material, which makes their comparison significant. Nanoparticles of $\text{Li}[\text{MnNi}]_2\text{O}_2$, $\text{Li}[\text{MnNiCo}]_2\text{O}_2$ layered and $\text{LiMn}_{1.5}\text{Ni}_{0.5}\text{O}_4$ spinel compounds as cathode materials were investigated. Fig. 13 shows the results of a typical comparison study of nano- and sub-micron structured $\text{LiMn}_{1/3}\text{Ni}_{1/3}\text{Co}_{1/3}\text{O}_2$ cathodes.⁸⁴ The XRD patterns in the figure and the SEM image reflect the nano-size of the active mass thus prepared in which the particle size calculated from the XRD peak width according to the Debye Scherer equation is reflected by the SEM images. Fig. 13 also shows typical voltage profiles of these materials measured vs. Li in EC-DMC/LiPF₆ at two different rates. As is

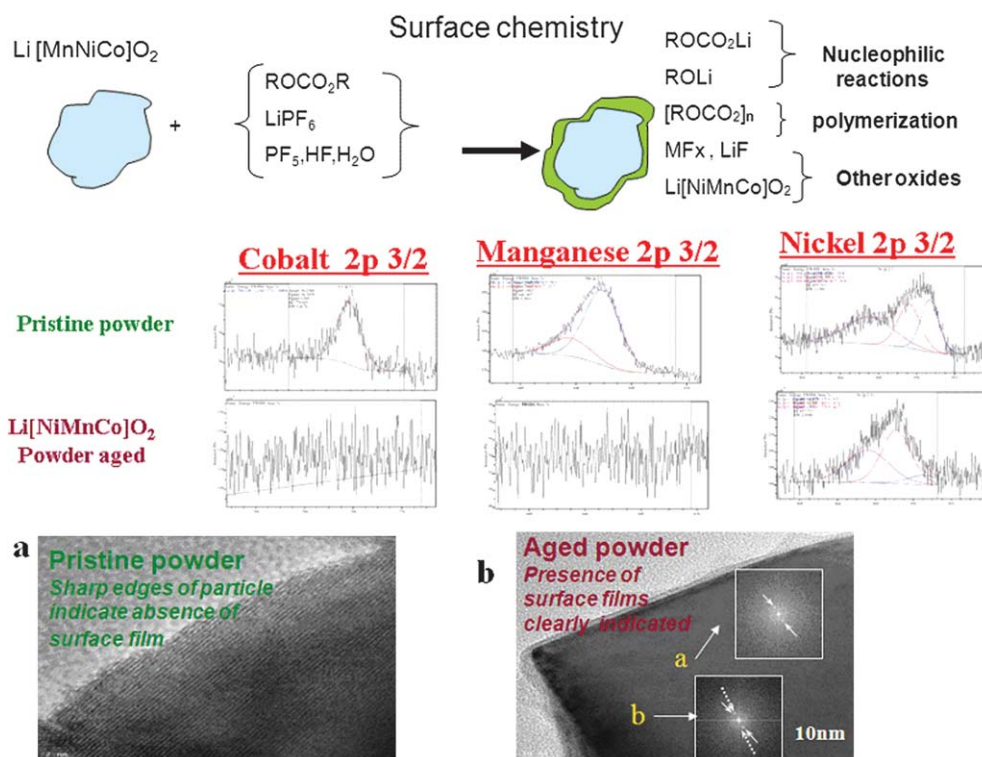


Fig. 14 A presentation related to the surface chemistry of Li[MnNiCo]O₂ particles. Upper part: a schematic presentation of core-shell structure formation due to surface reactions with solution species. Middle part: XPS spectra (Mn, Ni, Co) of pristine LiMn_{1/3}Ni_{1/3}Co_{1/3}O₂ particles compared to XPS spectra of particles after aging in EC-DMC/LiPF₆ solution. Lower part: HRTEM images of a pristine particle and a particle that was exposed during several weeks to ambient air.⁸⁵

seen in the CV, the voltage profiles of the electrodes comprising nanoparticles are less clean and reflect a lower rate capability as compared to the sub-micronic particles. This inferior rate capability of electrodes comprising nanoparticles, compared to the sub-micrometric active mass, is common to all cathodes comprising Li_xMO_y as the active mass. In fact, normally sub-micronic LiMn_{1/3}Ni_{1/3}Co_{1/3}O₂ materials show the highest rate capability and quite prolonged cycling as compared to other Li_xMO_y cathode materials. The reason for poor performance of the nanostructured analog is explained and illustrated in Fig. 14.^{9,12} The surface oxygens of lithiated TMOs are highly basic and nucleophilic. They react readily with acidic species (acid-base reactions) and with the electrophilic alkyl carbonate molecules. The nucleophilic attack on the alkyl carbonates by the surface oxygen anions likely initiate polymerization reactions that form surface polycarbonate species. The higher surface area of the 1000-fold smaller particles translates to a proportional increase in surface reactivity, and hence, nanoparticles of Li_xMnO₂ develop a core-shell structure of active material surrounded by a shell comprising both ionic and polymeric species (e.g., LiF, ROLi, ROCO₂Li, and polycarbonates). These surface layers lead to high impedances due to a slowed Li-ion migration through the surface films from solution to active mass. When these surface layers are too thick they also can interfere with interparticle electrical contact, worsening the electrical integrity of the composite electrodes. Both of these phenomena, as they relate primarily to the particle surfaces, are exacerbated in the nanostructured materials.

Fig. 14 presents a schematic view of the surface behavior and core-shell structure formation of Li_xMO₂ particles. HRTEM images of pristine and ambient-aged Li[MnNiCo]O₂ particles quite clearly indicate surface film formation as a sharp interface of the active mass at its surface is seen in the pristine material, while the particles aged in air are clearly seen to have a surface layer. The XPS data compare the Mn, Ni and Co spectra of pristine and aged (60 °C, EC-DMC/LiPF₆ solution) particles. As expected, the pristine data reflect the presence of the three transition metal atoms on the particles' surface in equal amounts. Upon aging, only Ni is detected, suggesting that subsequent surface reactions bury the Mn and Co, while Ni cations could still be found as part of ionic compounds such as NiF₂ and NiCO₃. This difference in the involvement of the transition metal cations in the surface reactions of Li[MnNiCo]O₂ particles correlates with the fact that Li_xNiO₂ is much more reactive towards standard electrolyte solution components than Li_xCoO₂ and Li_xMnO₂ compounds. Surface reactions of Li_xMO₂ with atmospheric CO₂ have also been demonstrated,⁸⁵ forming Li₂CO₃ as product *via* the delithiation of the active material with or without the involvement of atmospheric O₂, the latter reaction resulting in a third material phase.

Conclusion and summary

In conclusion the advanced cathode materials which indicate the most promise in bringing Li-ion battery technology one step further towards meeting the challenge of powering EVs include:

LiMn_{1.5}Ni_{0.5}O₄ spinel, Li₂MnO₃·LiMn_{1/3}Ni_{1/3}Co_{1/3}O₂ and LiMn_{0.8}Fe_{0.2}PO₄. Although significant work is still needed in order to complete their R&D, these cathode materials are much closer to meeting practical needs than any other advanced/novel systems (e.g., Li-air, Li-S, LiCoPO₄). Studies indicate that the best electrolyte solution remains the standard alkyl carbonate matrices, and the best performing current collector for these materials remains aluminium. In addition, minimal successes despite extensive work on alternative anode systems including Sn- and Si-based composites, their intermetallic compounds and nano-MO conversion reaction compounds reiterates the idea that graphite remains the most successful anode material for advanced Li-ion batteries. Surface modification of graphitic materials (e.g., by surface reactive additives in solutions) enables the enhancement of the stability of graphite anodes in prolonged cycling. It is important to develop new electrolyte systems with higher anodic stability than that of the standard electrolyte solutions, in order to substantiate the practical use of the advanced cathode materials described herein. Ionic liquids based on derivatives of cyclic quaternary ammonium cations may be considered as promising in this respect.

References

- 1 V. V. Seregin and R. B. Finkelman, *Int. J. Coal Geol.*, 2008, **76**, 253.
- 2 R. L. Hirsch, *Energy Policy*, 2008, **36**, 881.
- 3 S. Brown, D. Pyke and P. Steenhof, *Energy Policy*, 2010, **38**, 3797.
- 4 K. C. Divya and J. Ostergaard, *Electric Power Systems Research*, 2009, **79**, 511.
- 5 J. Larminie and A. Dicks, *Fuel Cell Systems Explained*, John Wiley & Sons, 2nd edn, 2003.
- 6 M. Felderhoff, C. Weidenthaler, R. V. Helmolt and U. Eberle, *Phys. Chem. Chem. Phys.*, 2007, **9**, 2643.
- 7 J. B. Goodenough and Y. Kim, *Chem. Mater.*, 2010, **22**, 587.
- 8 M. Ogasa, *IEEE Trans. Electr. Electron. Eng.*, 2008, **3**, 15.
- 9 L. Larush, V. Borgel, E. Markevich, O. Haik, E. Zinigrad, G. Semrau, M. Schmidt and D. Aurbach, *J. Power Sources*, 2009, **189**, 217.
- 10 E. Peled, Lithium Stability and Film Formation in Organic and Inorganic Electrolytes for Lithium Battery Systems, in *Lithium Batteries*, ed. J. P. Gabano, Academic press, London, 1983.
- 11 M. Moshkovich, M. Cojocaru, H. E. Gottlieb and D. Aurbach, *J. Electroanal. Chem.*, 2001, **497**, 84.
- 12 D. Aurbach, B. Markovsky, G. Salitra, E. Markevich, Y. Talyossef, M. Koltypin, L. Nazar, B. Ellis and D. Kovacheva, *J. Power Sources*, 2007, **165**, 491.
- 13 L. Wentao and B. L. Lucht, *J. Electrochem. Soc.*, 2006, **153**, A1617.
- 14 E. Markevich, G. Salitra and D. Aurbach, *Electrochem. Commun.*, 2005, **7**, 1298.
- 15 N. Kumagai, S. Komaba, Y. Kataoka and M. Koyanagi, *Chem. Lett.*, 2000, 1154.
- 16 S. K. Martha, H. Sclar, Z. Framovich, D. Kovacheva, N. Saliyski, Y. Gofer, P. Sharon, E. Golik, B. Markovsky and D. Aurbach, *J. Power Sources*, 2009, **189**, 248.
- 17 D. Aurbach, B. Markovsky, B. Rodkin, Y. Talyossef, G. Salitra and H. J. Kim, *J. Electrochem. Soc.*, 2004, **151**, A1068.
- 18 D. Aurbach, M. D. Levi and E. Levi, *Solid State Ionics*, 2008, **179**, 742.
- 19 C. P. Grey and Y. J. Lee, *Solid State Sci.*, 2003, **5**, 883.
- 20 O. Chusid and D. Aurbach, *J. Electrochem. Soc.*, 1993, **140**, L1.
- 21 K. Edström, T. Gustafsson and J. O. Thomas, *Electrochim. Acta*, 2004, **50**, 397.
- 22 (a) E. Markevich, V. Baranchugov, G. Salitra and D. Aurbach, *J. Electrochem. Soc.*, 2008, **155**, A132; (b) V. Baranchugov, E. Markevich, G. Salitra, M. Schmidt and D. Aurbach, *J. Electrochem. Soc.*, 2008, **155**, A217.
- 23 H. C. Choi and S. Y. Lee, *J. Phys. Chem. B*, 2002, **106**, 9252.
- 24 O. Haik, S. K. Martha, H. Sclar, Z. Samuk-Fromovich, E. Zinigrad, B. Markovsky, D. Kovacheva, N. Saliyski and D. Aurbach, *Thermochim. Acta*, 2009, **493**, 96.
- 25 Y. Cohen and D. Aurbach, *Rev. Sci. Instrum.*, 1999, **70**, 4668.
- 26 *Nonaqueous Electrochemistry*, ed. D. Aurbach and Y. Gofer, Marcel Dekker, Inc., New York, 1999, ch. 4.
- 27 P. Verma, P. Maire and P. Novák, *Electrochim. Acta*, 2010, **55**, 6332.
- 28 J. S. Gnanaraj, M. D. Levi and E. Levi, *J. Electrochem. Soc.*, 2001, **148**, A525.
- 29 N. Leifer, M. C. Smart, G. K. S. Prakash, L. Gonzalez, L. Sanchez, P. Bhalla, C. P. Grey and S. G. Greenbaum, *J. Electrochem. Soc.* In publication.
- 30 R. Marom, O. Haik, I. Halalay and D. Aurbach, *J. Electrochem. Soc.*, 2010, **157**, A972.
- 31 D. Aurbach and H. Gottlieb, *Electrochim. Acta*, 1989, **34**, 141.
- 32 K. Xu, *Chem. Rev.*, 2004, **104**, 4303.
- 33 A. Lewandowski and A. S. Mocek, *J. Power Sources*, 2009, **194**, 601.
- 34 D. Aurbach, V. Burgel, E. Markevich, G. Semrau and M. Schmidt, *J. Power Sources*, 2009, **189**, 331.
- 35 R. Sharaby, E. Markevich, V. Burgel, G. Semrau, M. Schmidt and D. Aurbach, *Electrochem. Solid-State Lett.*, 2010, **13**, A32.
- 36 Y. Talyossef, B. Markovsky, G. Salitra, D. Aurbach, H.-J. Kim and S. Choi, *J. Power Sources*, 2005, **146**, 664.
- 37 D. Aurbach, B. Markovsky, F. Amalraj, H. Gottlieb, Y. Gofer and S. Martha, *J. Electrochem. Soc.*, 2010, **157**, A423.
- 38 L. Hu, H. Wu, F. L. Mantia, Y. Yang and Y. Cui, *ACS Nano*, 2010, **4**, 5843.
- 39 H. K. Liu, Z. P. Guo, J. Z. Wang and K. Konstantinov, *J. Mater. Chem.*, 2010, **20**, 10055.
- 40 Z. Chen, Y. Cao, J. Qian, X. Ai and H. Yang, *J. Mater. Chem.*, 2010, **20**, 7266.
- 41 P. Poizot, S. Laruelle, S. Grugeon, L. Dupont and J. M. Tarascon, *Nature*, 2000, **407**, 496.
- 42 K. Amine, I. Belharouak, Z. Chen, T. Tran, H. Yumoto, N. Ota, S. T. Myung and Y. K. Sun, *Adv. Mater.*, 2010, **22**, 3052.
- 43 C. M. Park, J. H. Kim, H. Kim and H. J. Sohn, *Chem. Soc. Rev.*, 2010, **39**, 3115.
- 44 W. Wang, M. K. Datta and P. N. Kumta, *J. Mater. Chem.*, 2007, **17**, 3229.
- 45 M. Winter and J. O. Besenhard, *Electrochim. Acta*, 1999, **45**, 31.
- 46 C. K. Chan, R. N. Patel, M. J. O'Connell, B. A. Korgel and Y. Cui, *ACS Nano*, 2010, **4**, 1443.
- 47 P. L. Taberna, S. Mitra, P. Poizot, P. Simon and J.-M. Tarascon, *Nat. Mater.*, 2006, **5**, 567.
- 48 K.-S. Park, A. Benayad, D.-J. Kang and S.-G. Doo, *J. Am. Chem. Soc.*, 2008, **130**, 14930.
- 49 D. Aurbach, B. Markovsky, K. Gamolsky, E. Levi and Y. Ein-Eli, *Electrochim. Acta*, 1999, **45**, 67.
- 50 M. Winter, J. O. Besenhard, M. E. Spahr and P. Novak, *Adv. Mater.*, 1998, **10**, 725.
- 51 D. Aurbach, H. Teller and E. Levi, *J. Electrochem. Soc.*, 2002, **149**, A1255.
- 52 D. Aurbach, M. Koltypin and H. Teller, *Langmuir*, 2002, **18**, 9000.
- 53 E. Markevich, G. Salitra, E. Polak and D. Aurbach, *J. Power Sources*, 2007, **174**, 1263.
- 54 R. Elazati, G. Salitra, E. Polak, J. Affinito, C. Scordilis-kelley and D. Aurbach, *J. Electrochem. Soc.*, 2009, **156**, A694.
- 55 R. Elazari, G. Salitra, Y. Tal Yosef, Y. Grinblat, C. Scordilis-Kelley, A. Xiao, J. Affinito and D. Aurbach, *J. Electrochem. Soc.*, 2010, **157**, A1131.
- 56 R. D. Rau, K. M. Abraham, G. F. Pearson, J. K. Suprenant and S. B. Brummer, *J. Electrochem. Soc.*, 1979, **126**, 523.
- 57 X. L. Ji, K. T. Lee and L. F. Nazar, *Nat. Mater.*, 2009, **8**, 500.
- 58 J. Hassoun and B. Scrosati, *Adv. Mater.*, 2010, **22**, 5198.
- 59 G. Grishkumar, B. McCloskey, A. C. Luntz, S. Swanson and W. Wilcke, *J. Phys. Chem. Lett.*, 2010, **1**, 2193.
- 60 N. Imanishi, S. Hasegawa, T. Zhang, A. Hirano, Y. Takedo and O. Yamamoto, *J. Power Sources*, 2008, **185**, 1392.
- 61 D. Zhang, R. Li, T. Huang and A. Yu, *J. Power Sources*, 2010, **195**, 1202.
- 62 K. M. Shaju and P. G. Bruce, *Dalton Trans.*, 2008, **40**, 5471.
- 63 J. C. Arrebola, A. Caballero, M. Cruz, L. Hernán, J. Morales and E. R. Castellón, *Adv. Funct. Mater.*, 2006, **16**, 1904.
- 64 Y. Talyossef, B. Markovsky, R. Lavi, G. Salitra, D. Kovacheva, M. Gorova, E. Zhecheva, R. Stoyanova and D. Aurbach, *J. Electrochem. Soc.*, 2007, **154**, A682.
- 65 G. Q. Liu, L. Wen and Y. M. Liu, *J. Solid State Electrochem.*, 2010, **14**, 2919.

- 66 C. S. Johnson, N. Li, C. Lefief, J. T. Vaughey and M. M. Thackeray, *Chem. Mater.*, 2008, **20**, 6095.
- 67 S.-H. Kang, P. Kempgens, S. Greenbaum, A. J. Kropf, K. Amine and M. M. Thackeray, *J. Mater. Chem.*, 2007, **17**, 2069.
- 68 F. Amalraj, J. Grinblat, N. Leifer, D. Kovacheva, M. Talianker, L. Zeiri, G. Goobes, B. Markovsky and D. Aurbach, *J. Electrochem. Soc.*, 2010, **157**, A1121.
- 69 J. Cho, Y. W. Kim, B. Kim, J. G Lee and B. Park, *Angew. Chem., Int. Ed.*, 2003, **42**, 1618.
- 70 S. T. Myung, K. Izumi, S. Komaba, Y. K. Sun, H. Yashiro and N. Kumagai, *Chem. Mater.*, 2005, **17**, 3695.
- 71 Y. K. Sun, K. J. Hong, J. Prakash and K. Amine, *Electrochem. Commun.*, 2002, **4**, 344.
- 72 R. Dominko, M. Gaberscek, M. Bele, D. Mihailovic and J. Jamnik, *J. Eur. Ceram. Soc.*, 2007, **27**, 909.
- 73 A. K. Padhi, K. S. Nanjundaswamy and J. B. Goodenough, *J. Electrochem. Soc.*, 1997, **144**, 1188.
- 74 K.-S. Park, S. B. Schougaard and J. B. Goodenough, *Adv. Mater.*, 2007, **19**, 848.
- 75 Y. H. Huang and J. B. Goodenough, *Chem. Mater.*, 2008, **20**, 7237.
- 76 X. L. Wu, L. Y. Jiang, F. F. Cao, Y. G. Guo and L. J. Wan, *Adv. Mater.*, 2009, **21**, 2710.
- 77 T. Kojimaa, T. Ishizua, T. Horibaa and M. Yoshikawab, *J. Power Sources*, 2009, **189**, 859.
- 78 Z. Sun, G. Bebis and R. Miller, *IEEE Trans. Pattern Anal. Mach. Intell.*, 2006, **28**, 694.
- 79 S. Martha, B. Markovsky, I. Exnar and D. Aurbach, *J. Electrochem. Soc.*, 2009, **156**, A541.
- 80 D. Aurbach, S. Martha, B. Markovsky, O. Haik, E. Zinigrad and I. Exnar, *Angew. Chem., Int. Ed.*, 2009, **48**, 8559.
- 81 G. Chen and T. J. Richardson, *J. Power Sources*, 2010, **195**, 1221.
- 82 E. J. Plichta and W. K. Behl, *J. Power Sources*, 2000, **88**, 192.
- 83 D. Yaakov, I. C. Halalay and D. Aurbach, *J. Electrochem. Soc.*, 2010, **157**, A1383.
- 84 H. Sclar, D. Kovacheva, E. Zhecheva, R. Stoyanova, R. Lavi, G. Kimmel, J. Grinblat, O. Gershovitz, F. Amalraj, O. Heik, E. Zinigrad, B. Markovsky and D. Aurbach, *J. Electrochem. Soc.*, 2009, **156**, A938.
- 85 O. Haik, N. Leifer, Z. Framovich, E. Zinigrad, B. Markovsky, L. Larush, G. Goobes and D. Aurbach, *J. Electrochem. Soc.*, 2010, **157**, A1099.